


FULL PAPER

Direct synthesis of Fe(III) immobilized Zr-based metal–organic framework for aerobic oxidation reaction

Xin Shu¹  | Ying Yu¹ | Yi Jiang² | Yi Luan² | Daniele Ramella³

¹ College of Science, Beijing University of Chemical Technology, Beijing 100029, China

² School of Materials Science and Engineering, University of Science and Technology Beijing, 30 Xueyuan Road, Haidian District, Beijing 100083, China

³ Temple University-Beury Hall, 1901, N. 13th Street, Philadelphia, Pennsylvania 19122, USA

Correspondence

Xin Shu, College of Science, Beijing University of Chemical Technology, Beijing 100029.

Email: shuxin@mail.buct.edu.cn; yiluan@ustb.edu.cn

Funding information

BUCT Fund for Disciplines Construction and Development, Grant/Award Number: No. XK1529; Fundamental Research Funds for the Central Universities, Grant/Award Number: Grant No. FRF-TP-16-004A3; Beijing Natural Science Foundation, Grant/Award Number: Grant No. 2172037; National Natural Science Foundation of China, Grant/Award Number: No. 51503016

A Zr-based metal–organic framework with bipyridine units (UiO-67) has been utilized for the immobilization of catalytically active iron species via a post-synthetic metalation method. UiO-67 bipyridine MOF was synthesized through a simple solvothermal method and was shown to have a UiO-type structure. Post-synthetic metalation of UiO-67 MOF was performed for the immobilization of the catalytically active FeCl₃. FT-IR and EDX element map suggested that FeCl₃ is coordinately bonded to the UiO-67 bipyridine framework. The synthesized UiO-67-FeCl₃ catalyst was used for the aerobic oxidation of alcohols and benzylic compounds in the presence of molecular oxygen. In addition, the UiO-67-FeCl₃ catalyst can be reused as a solid heterogeneous catalyst without compromising its activity and selectivity.

KEYWORDS

alcohol oxidation, heterogeneous catalyst, iron(III) catalyst, metal-organic framework, molecular oxygen

1 | INTRODUCTION

Transformation of alcohols to the corresponding carbonyl compounds is an important chemical reaction in organic synthetic chemistry.^[1] In the past decade, tremendous efforts have been devoted to the development of homogeneous catalysts for alcohol oxidation.^[2] Stoichiometric amounts of oxidants, such as 2-iodoxybenzoic acid (IBX), *m*-chloroperbenzoic acid (*m*-CPBA) and organic peroxides have been utilized in oxidation reactions with quite high activity.^[3] On the other hand, a catalytic oxidation process employing molecular oxygen would be highly desirable to avoid toxic and hazardous stoichiometric oxidants. Molecular oxygen is inexpensive, safe and abundant, and it only generates clean by-products.^[4] For this reason, several studies have

focused on utilizing molecular oxygen as the oxidant in homogeneous, catalytic, and aerobic oxidation reactions.^[5] Noble metal particles or complexes have been reported as good homogeneous oxidation catalysts.^[6] However, inexpensive transition metals, such as cobalt, iron, and copper were preferred as great replacements of noble metals.^[7] The catalysis field has witnessed the development of the homogeneous iron and copper catalysts in combination with 2,2,6,6-tetramethylpiperidine-N-oxyl (TEMPO) for the selective oxidation of alcohols using molecular oxygen.^[8] However, despite having high activity, these catalysts suffered from inherent problems during the separation, deactivation, and recycling steps.

To overcome these issues, heterogeneous iron catalysts for aerobic oxidation of alcohols have been explored. Metal

complexes anchored on solid supports, such as polymers^[9] and mesoporous silica, have been developed.^[10] Recently, metal–organic frameworks (MOFs) have emerged as a new class of heterogeneous catalysts thanks to their highly tailorable nature, porous structure and large surface area.^[11] Post-synthetic metalation (PSM) of porous MOFs could introduce transitional metal moieties to the MOF structure through coordinative interactions; this is highly convenient for transition metal mediated catalysis.^[12] Several literature reports utilized MOF structure modifications for the rapid introduction of *N*-containing functional groups.^[13] However, these reported methods usually take more than one-step for the synthesis of functionalized MOFs. Several literature report utilized the bipyridine moiety on MOF structure for the immobilization of transitional metals.^[14]

In this work, we wish to report a novel iron immobilized bipyridine MOF catalyst, which enables the development of efficient and recyclable heterogeneous oxidation catalysis. A Zr-based metal–organic framework with bipyridine units (UiO-67) was synthesized by a simple solvothermal method and was shown to have a UiO-type structure. The Zr-based UiO-67 MOF was achieved with an organic linker of 2,2'-bipyridine-5,5'-dicarboxylic acid, which serves as an excellent organic ligand in the formation of the iron complex. The synthesized UiO-67-FeCl₃ catalyst served as an efficient catalyst for aerobic oxidation reaction. Then this methodology was further extended to the benzylic oxidation using oxygen as the oxidant.^[15] Lastly, the pyridine moiety on the UiO-67 bipyridine MOF can also serve as an organic additive during the oxidation process.

2 | EXPERIMENTAL SECTION

2.1 | Materials

All the chemicals were used without further purification.

2.2 | Preparation of UiO-67 metal–organic framework

A Zr-based MOF with an organic linker of 2,2'-bipyridine-5,5'-dicarboxylic acid (UiO-67) was prepared solvothermally according to published procedures.^[16] The UiO-67 crystals were precipitated, filtered, washed repeatedly with methanol, and dried at room temperature for 24 h.

2.3 | Preparation of UiO-67-FeCl₃ catalyst

UiO-67 (100 mg) and FeCl₃·6H₂O (87 mg) were added to acetonitrile (15 ml), and the mixture was heated at 313 K in air. The solid powder was collected by filtration and dried under vacuum. The synthesized UiO-67-FeCl₃ was analyzed by ICP-AES prior to use.

2.4 | Catalytic selective oxidation of alcohols

In general, the catalytic reaction was carried out under the following conditions: 5 mol% UiO-67-FeCl₃ catalyst (based on iron), 0.1 mmol additive, 0.2 mmol of 2,2,6,6-tetramethylpiperidine-*N*-oxyl (TEMPO) and 1.0 mmol alcohol were mixed in 2.5 ml of CH₃CN. The air in the above reaction system was evacuated and oxygen gas was supplied through a balloon. After each catalytic cycle, the solution was centrifuged and the filtered liquid solution was analyzed via gas chromatography–mass spectrometry using nitrobenzene as the internal standard.

2.5 | Catalytic selective oxidation of benzylic compounds

In general, the catalytic reaction was carried out under the following conditions: 5 mol% UiO-67-FeCl₃ catalyst (based on iron), 0.1 mmol NaNO₂, 0.2 mmol of TEMPO and 1.0 mmol benzylic compound were mixed in 2.5 ml of CH₃CN. The reaction was stirred at 60 °C for 24 h under 1 atmosphere of O₂. The air in the above reaction system was evacuated and oxygen gas was supplied through a balloon. After each catalytic cycle, the solution was centrifuged and the filtered liquid solution was analyzed via gas chromatography–mass spectrometry using nitrobenzene as the internal standard.

2.6 | Leaching test

The UiO-67-FeCl₃ catalyst was filtered after 4 h reaction time, the conversion of benzyl alcohol and selectivity of benzaldehyde was tested by GC/MS using nitrobenzene as the internal standard. The mixture was further stirred for an additional 8 h. After the reaction, the products were analyzed by GC/MS using nitrobenzene as the internal standard.

3 | RESULTS AND DISCUSSION

The crystalline structure of UiO-67 was evidenced by scanning electron microscopy (SEM) in Figure 1. UiO-67 crystals appear to be cubic morphology at the size of 1.5 μm diameters (Figure 1a). Cubic crystals of UiO-67 were well dispersed according to the SEM images. UiO-67-FeCl₃ was prepared by treating UiO-67 with FeCl₃·6H₂O (Scheme 1). The structural morphology was maintained under the acidic FeCl₃·6H₂O condition as shown in Figure 1b.

The EDX elemental maps verified the successful incorporation of FeCl₃·6H₂O and the iron was well dispersed in and on the surface of UiO-67 (Figure 2). The iron and chlorine elemental maps of the UiO-67-FeCl₃ particles showed an excellent distribution of FeCl₃ among all the particles. This

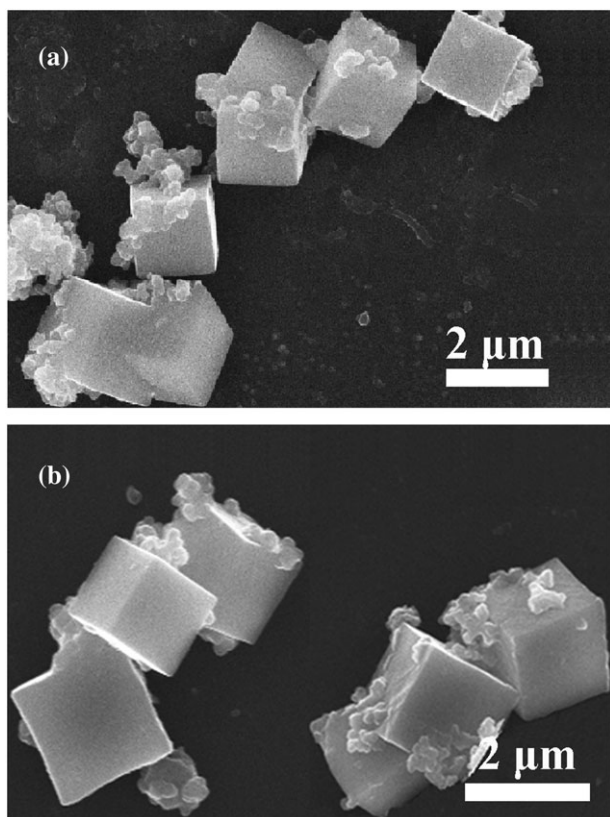
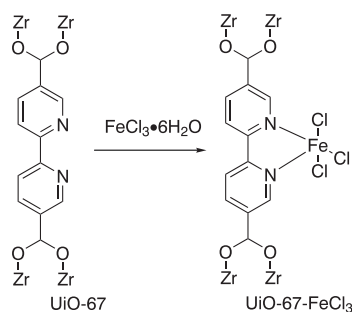


FIGURE 1 SEM images of (a) UiO-67 and (b) UiO-67-FeCl₃



SCHEME 1 Schematic illustration of the UiO-67-FeCl₃ synthesis

observation fits our expectation as well distributed iron(III) possesses high catalytic efficiency.

The structural integrity of the UiO-67 and UiO-67-FeCl₃ catalysts was proved by powder X-ray diffraction (pXRD) (Figure 3). The pXRD spectrum of UiO-67 revealed the great crystalline structure of the UiO-67 material, which is in agreement with the literature (Figure 3a).^[17] The powder XRD pattern for UiO-67-FeCl₃ indicated a high similarity of UiO-67 and UiO-67-FeCl₃ in terms of the main framework, formed by a zirconium cluster and 2,2'-bipyridine carboxylate ligand (Figure 3b). Evidence of FeCl₃ complex formation for the UiO-67-FeCl₃ material was further provided by the FT-IR spectra shown in Figure S1. A strong peak at 1610 cm⁻¹ indicated a large amount of carboxylate

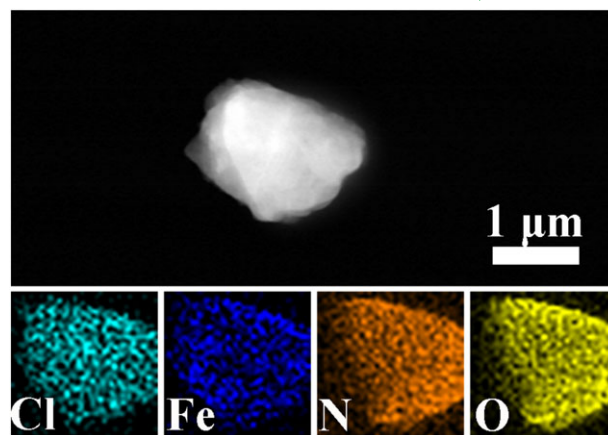


FIGURE 2 The TEM images of the UiO-67-FeCl₃ and EDX elemental maps of Cl, Fe, N and O, respectively

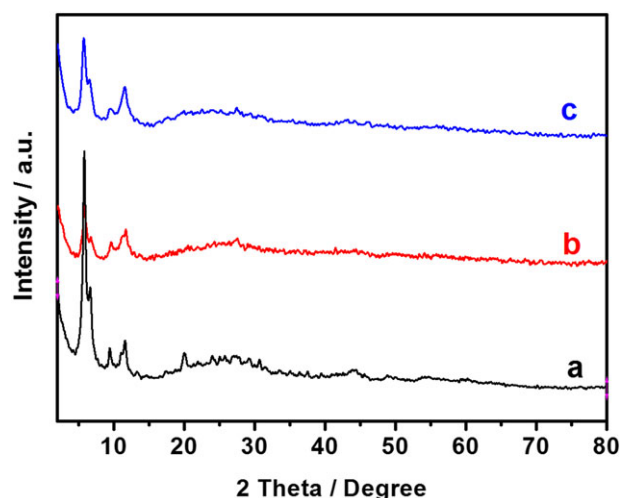


FIGURE 3 XRD patterns of (a) UiO-67, (b) UiO-67-FeCl₃ and (c) recycled UiO-67-FeCl₃

functional group. However, no significant new peak was observed for UiO-67-FeCl₃ when compared with its UiO-67 precursor, presumably because of the relatively low loading of iron content (Figure S1).

The immobilization of iron content was further characterized by X-ray photoelectron spectroscopy (XPS). XPS measurements were performed for UiO-67 and UiO-67-FeCl₃ to further investigate coordination environments. The binding energy of the N 1s peak of UiO-67 (at around 398.7 eV) was shifted toward higher binding energy (at around 399.3 eV) after the FeCl₃ coordination (Figure 4 and 5). It is postulated that this observed N 1s peak shift is attributed to a decrease in the electron density of the N atom due to the N[⋯]Fe coordination. The peak of iron was detected in the XPS spectra UiO-67-FeCl₃, which further confirmed the introduction of Fe³⁺ content (Figure 5).^[18]

The thermal stability of the UiO-67 and UiO-67-FeCl₃ MOFs materials was examined by the thermal gravimetric analysis (TGA) in the temperature range of 50-1000 °C.

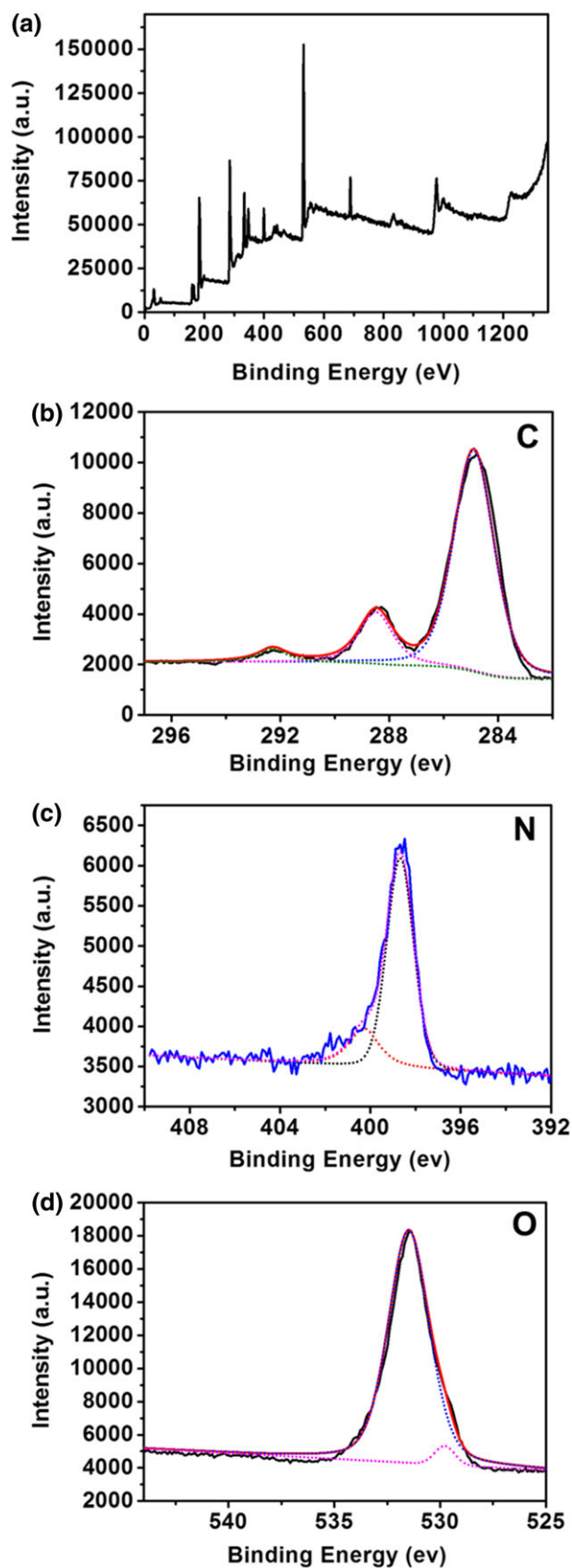
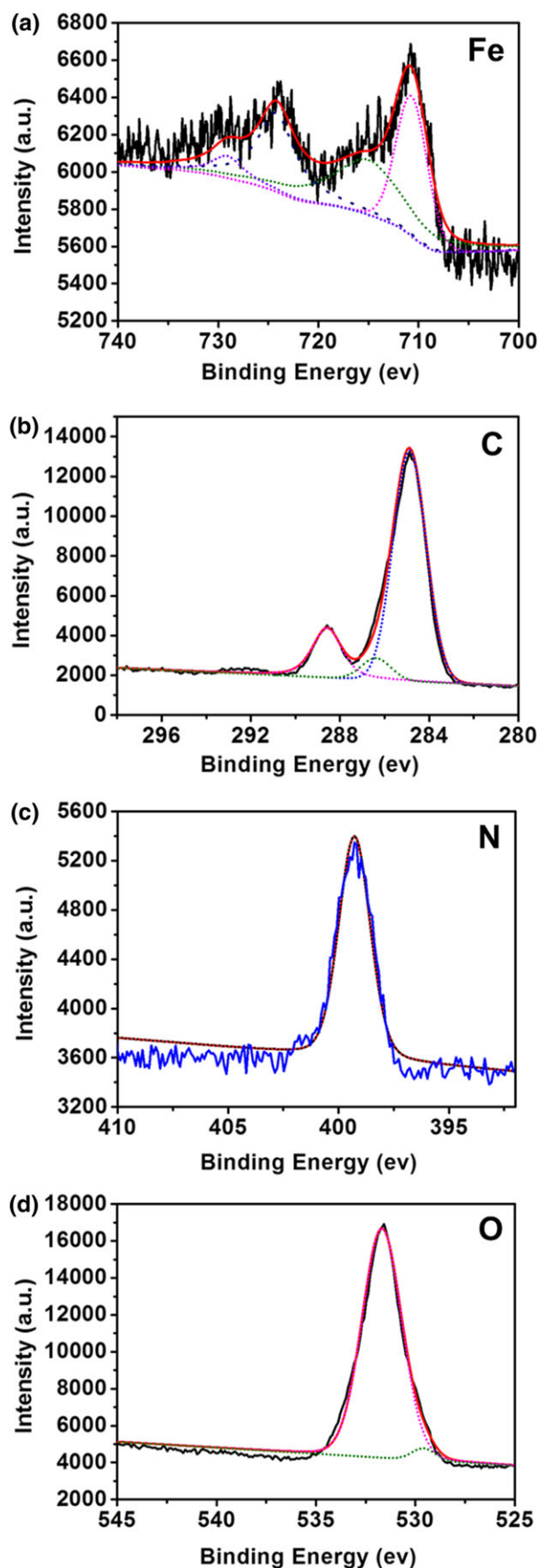


FIGURE 4 XPS spectra of UiO-67

FIGURE 5 XPS spectra of UiO-67-FeCl₃

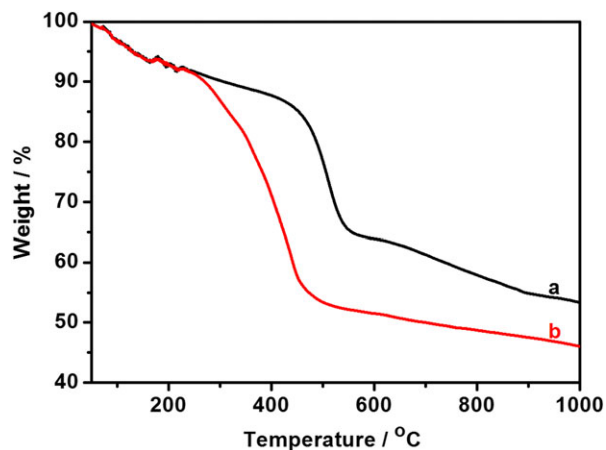


FIGURE 6 TGA of (a) UiO-67 and (b) UiO-67-FeCl₃

The initial weight loss between 50 °C and 100 °C was due to the loss of moisture. The framework of UiO-67 started to degrade from 425 °C and the framework decomposition ended at 550 °C (Figure 6a). As for UiO-67-FeCl₃, a weight loss was observed at 275 °C and it ended at 475 °C (Figure 6b). The introduction of FeCl₃ reduced the thermal stability of UiO-67 MOF material. However, the TGA results suggested that the UiO-67-FeCl₃ catalyst is thermally stable under the aerobic oxidation reaction conditions.

UiO-67 is a highly porous MOF material with a BET surface area of 1614 m² g⁻¹, calculated by nitrogen adsorption isotherms collected for the UiO-67 MOF (Figure 7). After post-synthetic metalation, UiO-67-FeCl₃ has a calculated surface area of 624 m² g⁻¹, which is lower than that of its MOF precursor. It is expected that post-synthetic metalation of UiO-67 would result in a decrease in BET surface area since the introduction of the FeCl₃ moiety causes the occupation of the porous structure. However, the flexibility of the newly introduced FeCl₃ allows the free entry and exit of the alcohol substrate. In this way, the reduced surface area has limited negative impact on the catalytic activities. The pore

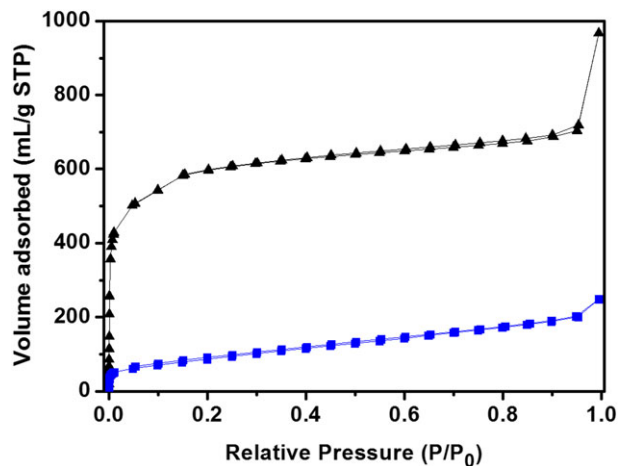


FIGURE 7 N₂ adsorption/desorption of UiO-67 (top, black) and UiO-67-FeCl₃ (bottom, blue)

size and pore volume before and after FeCl₃ immobilization were calculated by BJH method. The pore size of UiO-67 was calculated to be 1.23 nm, while UiO-67-FeCl₃ has two sets of pore of 0.95 and 1.18 nm (Fig. S2 and S3). The pore volume of UiO-67 is 1.015 cm³/g, while the pore volume of UiO-67-FeCl₃ was reduced to 0.389 cm³/g. In addition, the amount of FeCl₃ introduced was analyzed by ICP-AES of iron element. The percent weight of iron was determined to be 5.4 wt%. The ICP-AES result is used for the addition of iron derived heterogeneous UiO-67-FeCl₃ catalyst.

To evaluate the catalytic performance of the UiO-67-FeCl₃ catalysts, the aerobic oxidation of benzyl alcohol was chosen as a model reaction and the results are summarized in Table 1. No benzyl alcohol conversion was observed in the absence of the catalyst (Table 1, entry 1). Homogeneous FeCl₃·6H₂O showed good yields in the presence of 50 mol% of NaNO₂ additive (Table 1, entry 2). The yield was significantly compromised when only 10 mol% of NaNO₂ additive with 5 mol% of FeCl₃·6H₂O (Table 1, entry 3) were added. NaHCO₃ was also tested as an additive in the aerobic oxidation reaction and it gave a less satisfying yield of the desired aldehyde product (Table 1, entries 4–5). The UiO-67 MOF was tested to confirm there is no background reaction promoted by Zr-derived MOF. There is almost no alcohol conversion observed for UiO-67 MOF (Table 1, entry 6). As for iron immobilized UiO-67-FeCl₃ catalyst, 99% yield of benzaldehyde was achieved when a stoichiometric amount of NaNO₂ was used (Table 1, entry 7). This observation confirmed that

TABLE 1 Reaction optimization of aerobic oxidation reaction^a

Entry	Catalyst	Additive (mol%)	Solvent	Yield ^b
1	-	NaNO ₂ (100 mol%)	CH ₃ CN	<5%
2	FeCl ₃ ·6H ₂ O	NaNO ₂ (50 mol%)	CH ₃ CN	99%
3	FeCl ₃ ·6H ₂ O	NaNO ₂ (10 mol%)	CH ₃ CN	67%
4	FeCl ₃ ·6H ₂ O	NaHCO ₃ (50 mol%)	CH ₃ CN	75%
5	FeCl ₃ ·6H ₂ O	NaHCO ₃ (10 mol%)	CH ₃ CN	25%
6	UiO-67	NaNO ₂ (100 mol%)	CH ₃ CN	<5%
7	UiO-67-FeCl ₃	NaNO ₂ (100 mol%)	CH ₃ CN	99%
8	UiO-67-FeCl ₃	NaNO ₂ (50 mol%)	CH ₃ CN	99%
9	UiO-67-FeCl ₃	NaNO ₂ (10 mol%)	CH ₃ CN	99%
10	UiO-67-FeCl ₃	NaHCO ₃ (10 mol%)	CH ₃ CN	87%
11	UiO-67-FeCl ₃	NaNO ₂ (10 mol%)	PhCH ₃	91%
12	UiO-67-FeCl ₃	NaNO ₂ (10 mol%)	THF	73%
13	UiO-67-FeCl ₃	NaNO ₂ (10 mol%)	EtOH	54%

^aReaction conditions: alcohol (1.0 mmol), Fe catalyst (0.05 mmol), additive, TEMPO (0.2 mmol) in solvent (2.5 ml) for 12 h at room temperature, the yield was determined by GC-MS using nitrobenzene as the internal standard

TABLE 2 Aerobic oxidation of alcohols using UiO-67-FeCl₃ catalyst

Entry	Substrate	Product	Sel.	GC Yield	Isolated Yield
1			99%	99%	95%
2			99%	93%	88%
3			99%	99%	99%
4			99%	95%	95%
5			99%	95%	94%
6			99%	98%	92%
7			99%	87%	81%
8			99%	67%	63%
9			99%	58%	52%

Reaction conditions: alcohol (1.0 mmol), UiO-67-FeCl₃ (0.05 mmol), NaNO₂ (0.1 mmol), TEMPO (0.2 mmol), CH₃CN (2.5 mL) were stirred at room temperature for 12 h under 1 atmosphere of O₂

FeCl₃ is responsible for the catalytic activity. When the amount of NaNO₂ was lowered while using UiO-67-FeCl₃ instead, the yield remained excellent. It is postulated that the pyridine moiety of the UiO-67 framework serves as an organic base, which facilitates the conversion of benzyl alcohol (Table 1, entries 8–9). Acetonitrile (CH₃CN), toluene (PhCH₃), tetrahydrofuran (THF) and ethanol solvents were screened and yield to benzaldehyde of 99%, 91%, 73% and 54%, respectively, were measured. A variety of solvents were tested using the UiO-67-FeCl₃ catalyst as well (Table 1, entries 11–13). The solvent screening indicated that CH₃CN was the most suitable solvent for the UiO-67-FeCl₃-catalyzed oxidation reaction. It can be concluded that the UiO-67-FeCl₃ catalyst, in combination with 10 mol% of NaNO₂ and 20 mol % of TEMPO in acetonitrile are the optimal reaction conditions for the oxidation of aromatic alcohols.

Under the optimal reaction conditions, the UiO-67-FeCl₃ catalyst was evaluated to prove its general applicability towards a variety of alcohol substrates (Table 2). An aromatic alcohol with a *para*-electron-donating group, 4-methoxybenzyl alcohol **1b**, was converted to its corresponding aldehyde **2b** in 99% yield (Table 2, entry 1). 4-Fluorobenzyl alcohol **1c**, which bears a *para*-electron-withdrawing group, showed a slightly compromised yield of the desired aldehyde **2c** (Table 2, entry 2). The heteroaromatic alcohol **1d** was also compatible with this system, providing the corresponding picolinaldehyde **2d** in 99% yield (Table 2, entry 3). In addition, 3-phenyl-1-propen-1-ol **1f** was evaluated as an enol and 92% yield was achieved (Table 2, entry 4). Aerobic oxidation reactivity is maintained for activated heterocycles alcohols of furan and thiophene (Table 2, entries 5–6). They both gave the desired aldehyde products **2g** and **2h** in over 95% yield. Secondary benzylic alcohol **1i** was converted to its corresponding oxidation product benzyl **2i**

TABLE 3 Oxidation of the benzylic position of hydrocarbon derivatives using UiO-67-FeCl₃ catalyst

Entry	Substrate	Product	Sel.	GC Yield	Isolated Yield
1			98%	92%	90%
2			99%	>99%	99%
3			99%	>99%	99%

Reaction conditions: benzylic compound (1.0 mmol), UiO-67-FeCl₃ (0.05 mmol), NaNO₂ (0.1 mmol), TEMPO (0.2 mmol), CH₃CN (2.5 ml) were stirred at 60 °C for 24 h under 1 atmosphere of O₂

in good yield (Table 2, entry 7). Furthermore, 1-phenylethanol **1j** and 1,2,3,4-tetrahydronaphthalen-1-ol **1k** were tested as secondary alcohols and 67% and 58% yields were observed, respectively (Table 2, entries 8–9).

The optimized oxidation reaction conditions were applied in the aerobic benzylic oxidation as the further extension of our methodology. Ethylbenzene **3a** was oxidized to acetophenone **2g** in 92% conversion and 98% selectivity (Table 3, entry 1). By oxidation of 9*H*-fluorene **3b**, the reaction proceeded smoothly to form fluorenone **2h** with excellent results (Table 3, entry 2). Then the oxidation of di(4-fluorophenyl)methane **3c** to 4,4'-difluorobenzophenone **2i** went smoothly in high yield (Table 3, entry 3). These results demonstrated the great generality of our UiO-67-FeCl₃ oxidation methodology.

The recyclability and reusability of UiO-67-FeCl₃ catalyst was also tested using benzyl alcohol oxidation as the model reaction. The solid UiO-67-FeCl₃ catalyst was centrifuged after each cycle, then washed with CH₃CN three times and vacuum dried at 40 °C. The recovered UiO-67-FeCl₃ catalyst retained excellent efficiency and selectivity after five reaction cycles (Figure 8). In addition, the supernatant liquid of the CH₃CN suspension showed no catalytic reactivity toward the benzyl alcohol, which supports the hypothesis that no leakage of UiO-67-FeCl₃ catalyst happens. Furthermore, the hot filtration test was performed and the result is shown in Figure 9. Two sets of experiments were performed under the same catalytic condition using benzyl alcohol as the model substrate. Both of reaction were run 12 h total, except the second reaction (red curve) was paused for the removal of solid catalyst. Each of the reaction was analyzed every 2 h for the determination of selectivity and yield. After the solid UiO-67-FeCl₃ catalyst was isolated from the reaction system at 4 h, the conversion of benzyl alcohol paused. This observation suggested no significant leakage of FeCl₃

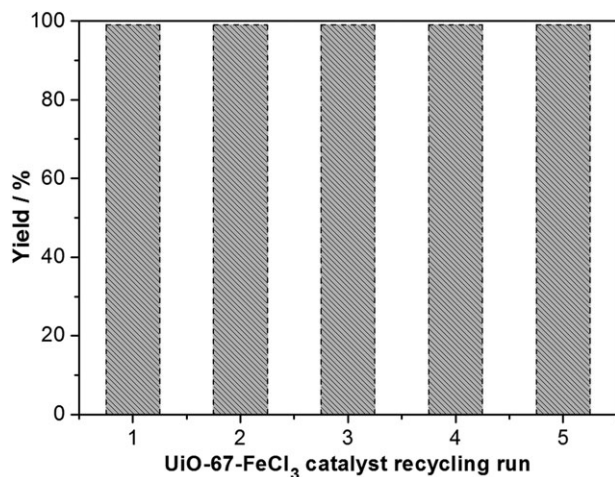


FIGURE 8 UiO-67-FeCl₃ catalyst recycle use for benzyl alcohol oxidation

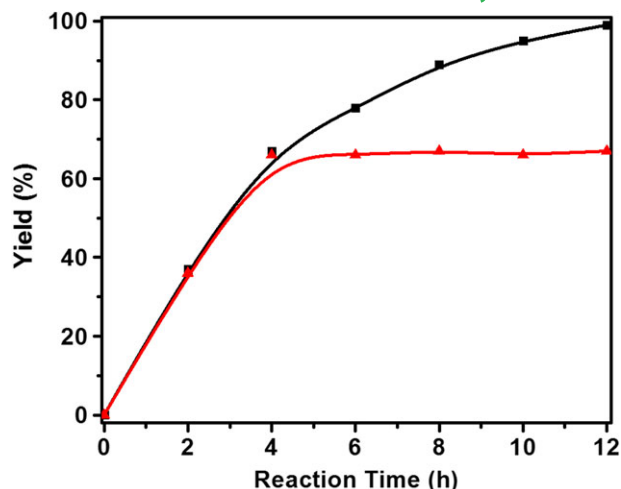


FIGURE 9 Hot filtration test and benzyl alcohol conversion versus time curve

content occurred during the oxidation process. The inductively coupled plasma atomic absorption spectroscopy (ICP-AES) analysis of the filtrate gave an iron content of 6.3 ppm, which also indicated that the leaching of iron into the solvent was negligible during the reaction. Lastly, the powder XRD pattern and FT-IR spectra showed no significant differences between fresh UiO-67-FeCl₃ catalyst and the one isolated after five cycles (Figure 3c and S1). These results suggested the high stability of our UiO-67-FeCl₃ catalyst under the oxidation reaction conditions.

A plausible mechanism of UiO-67-FeCl₃ promoted aerobic oxidation can be described as a cascade of redox reactions involving two cycles in Figure 10. The role of TEMPO is to carry out the main oxidation reaction of alcohols assisted by Fe³⁺ that initiates electron and proton transfer step in cycle I where Fe(III) species is reduced to generate Fe(II) species. NaNO₂ is a source of NO₂, which is responsible to the oxidation of Fe(II) species to Fe(III) species and NO₂ is reduced to NO. In the meanwhile, the cycle II oxidation process involves the oxidation of Fe(II) to Fe(III) by NO₂ and the oxidation of TEMPOH to TEMPO by Fe(III). In summary,

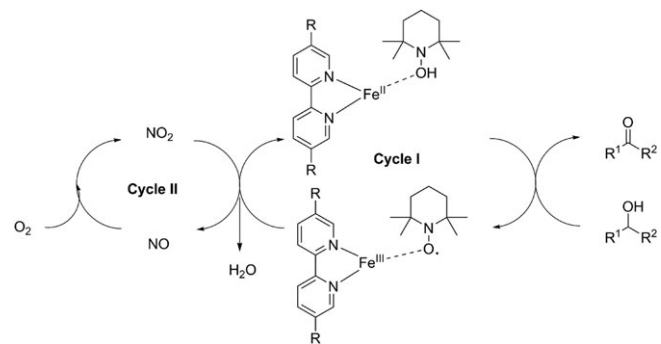


FIGURE 10 Proposed mechanism for the aerobic oxidation of alcohols

the oxidation of NO to NO₂ can be easily carried out in the presence of molecular oxygen.

4 | CONCLUSIONS

In conclusion, a Zr-based MOF with an organic linker of 2,2'-bipyridine-5,5'-dicarboxylic acid (UiO-67) was prepared solvothermally. A novel UiO-67-FeCl₃ catalyst was synthesized by treating UiO-67 with FeCl₃·6H₂O. Then the UiO-67-FeCl₃ was utilized as an efficient catalyst for the promotion of aerobic oxidation of alcohols and aerobic benzylic oxidations. The pyridine moiety of the UiO-67-FeCl₃ catalyst also served as an organic base, which allowed the amount of basic additive to be reduced. A variety of alcohols were tested and converted to their corresponding ketones in good yields. In addition, similar reaction conditions were extended to the aerobic oxidation of benzylic carbons to phenones, using molecular oxygen as the oxidant. The initial catalytic activity of the UiO-67-FeCl₃ catalyst was maintained after five consecutive reaction cycles. Hot filtration tests and ICP-AES analyses of the solution suggested the extremely low leakage of the iron content during the reaction process. Further studies will aim at extending the applications of these MOF catalysts to the oxidation of other substrates.

ACKNOWLEDGEMENTS

We thank the Beijing Municipal Natural Science Foundation (Grant No. 2172037), the National Natural Science Foundation of China (No. 51503016) and Fundamental Research Funds for the Central Universities (Grant No. FRF-TP-16-004A3) for financial support. Xin Shu also thanks BUCT Fund for Disciplines Construction and Development (No. XK1529) for financial support.

REFERENCES

- [1] Q. Cao, L. M. Dornan, L. Rogan, N. L. Hughes, M. J. Muldoon, *Chem. Commun.* **2014**, 50, 4524.
- [2] C. Parmeggiani, F. Cardona, *Green Chem.* **2014**, 14, 547.
- [3] a) A. Xie, X. Zhou, L. Feng, X. Hu, W. Dong, *Tetrahedron* **2014**, 70, 3514. b) N. Gunasekaran, P. Jerome, S. W. Ng, E. R. T. Tierink, R. Karvembu, *J. Mol. Catal. A-Chem.* **2012**, 353, 156.
- [4] Y. Qi, Y. Luan, J. Yu, X. Peng, G. Wang, *Chem. – Eur. J.* **2015**, 21, 1589.
- [5] S. E. Allen, R. R. Walvoord, R. Padilla-Salinas, M. C. Kozlowski, *Chem. Rev.* **2013**, 113, 6234.
- [6] M. Stratakis, H. Garcia, *Chem. Rev.* **2012**, 112, 4469.
- [7] a) J. M. Hoover, B. L. Ryland, S. S. Stahl, *ACS Catal.* **2013**, 3, 2599. b) M. F. Semmelhack, C. R. Schmid, D. A. Cortes, C. S. Chou, *J. Am. Chem. Soc.* **1984**, 106, 3374.
- [8] a) L. Y. Wang, J. Li, Y. Lv, G. D. Zhao, S. Gao, *Appl. Organomet. Chem.* **2012**, 26, 37. b) N. Wang, R. Liu, J. Chen, X. Liang, *Chem. Commun.* **2005**, 42, 5322. c) J. M. Hoover, S. S. Stahl, *J. Am. Chem. Soc.* **2011**, 133, 16901.
- [9] a) P. R. Likhari, R. Arundhathi, S. Ghosh, M. L. Kantam, *J. Mol. Catal. A-Chem.* **2009**, 302, 142. b) M. A. Chari, K. Syamasundar, *Synthesis* **2005**, 5, 708.
- [10] J. Mao, X. Hu, H. Li, Y. Sun, C. Wang, Z. Chen, *Green Chem.* **2008**, 10, 827.
- [11] S. M. Cohen, *Chem. Sci.* **2010**, 1, 32.
- [12] a) J. D. Evans, C. J. Sumbly, C. J. Doonan, *Chem. Soc. Rev.* **2014**, 43, 5933. b) K. Manna, T. Zhang, W. Lin, *J. Am. Chem. Soc.* **2014**, 136, 6566. c) A. Dhakshinamoorthy, A. M. Asiri, H. Garcia, *Chem. – Eur. J.* **2016**, 22, 8012. d) A. Dhakshinamoorthy, M. Alvaro, H. Garcia, *Catal. Sci. Technol.* **2011**, 1, 856.
- [13] a) C. J. Doonan, W. Morris, H. Furukawa, O. M. Yaghi, *J. Am. Chem. Soc.* **2009**, 131, 9492. b) J. Canivet, S. Aguado, Y. Schuurman, D. Farrusseng, *J. Am. Chem. Soc.* **2013**, 135, 4195.
- [14] a) H. Duan, M. Li, G. Zhang, J. R. Gallagher, Z. Huang, Y. Sun, Z. Luo, H. Chen, J. T. Miller, R. Zou, A. Lei, Y. Zhao, *ACS Catal.* **2015**, 5, 3752. b) S. Øien, G. Agostini, S. Svelle, E. Borfecchia, K. A. Lomachenko, L. Mino, E. Gallo, S. Bordiga, U. Olsbye, K. P. Lillerud, C. Lamberti, *Chem. Mater.* **2015**, 27, 1042. c) P. Neves, A. C. Gomes, T. R. Amarante, F. A. A. Paz, M. Pillinger, I. S. Gonçalves, A. A. Valente, *Microporous Mesoporous Mater.* **2015**, 202, 106. d) P. Valvekens, E. D. Bloch, J. R. Long, R. Ameloot, D. E. De Vos, *Catal. Today* **2015**, 246, 55. e) K. Leus, Y. Y. Liu, M. Meledina, S. Turner, G. Van Tendeloo, P. Van Der Voort, *J. Catal.* **2014**, 316, 201. f) Y. Y. Liu, R. Decadt, T. Bogaerts, K. Hemelsoet, A. M. Kaczmarek, D. Poelman, M. Waroquier, V. Van Speybroeck, R. Van Deun, P. Van der Voort, *J. Phys. Chem. C* **2013**, 117, 11302. g) A. E. Platero-Prats, A. B. Gómez, L. Samain, X. Zou, B. Martín-Matute, *Chem. – Eur. J.* **2015**, 21, 861.
- [15] K. Chen, P. Zhang, Y. Wang, H. Li, *Green Chem.* **2014**, 16, 2344.
- [16] H. Feia, S. M. Cohen, *Chem. Commun.* **2014**, 50, 4810.
- [17] T. Toyao, K. Miyahara, M. Fujiwaki, T. H. Kim, S. Dohshi, Y. Horiuchi, M. Matsuoka, *J. Phys. Chem. C* **2015**, 119, 8131.
- [18] Y. Zhang, Z. X. Zhang, T. B. Li, X. G. Liu, B. S. Xu, *Spectrochim. Acta A* **2008**, 70, 1060.

SUPPORTING INFORMATION

Additional Supporting Information may be found online in the supporting information tab for this article.

How to cite this article: Shu X, Yu Y, Jiang Y, Luan Y, Ramella D. Direct synthesis of Fe(III) immobilized Zr-based metal–organic framework for aerobic oxidation reaction. *Appl Organometal Chem.* 2017;e3862. <https://doi.org/10.1002/aoc.3862>